

MICROCOPY RESOLUTION TEST CHART
NATIONAL BUREAU OF STANDARDS-1963-A

AD-A181 001

EFFECT OF GAS BUBBLES ON THE PLASTIC
ZONE AROUND A CRACK TIP

Guido D.C. Dhondt
A. Cemal Eringen

April 1987

U.S. Army Research Office
Contract DAAL03-86-K-0019

Princeton University

APPROVED FOR PUBLIC RELEASE:
DISTRIBUTION UNLIMITED

The findings in this report are not to be
construed as an official Department of the
Army position, unless so designated by
other authorized documents.

DTIC
SELECTED
JUN 01 1987

*

E

Figure captions.

fig 1: gas bubble around a crack tip.

fig 2: tension regions for a gas bubble around a crack tip.

fig 3: mode-I crack with a line distribtuion of edge dislocations.

fig 4: mode-I crack with two symmetric line distribtuions of edge dislocations.

Fig 5: Plastic zone with distance of the gas bubble from the crack tip ($\alpha = 55^\circ$).

Fig 6: Plastic zone with distance of the gas bubble from the crack tip ($\alpha = 60^\circ$).

Fig 7: Plastic zone with distance of the gas bubble from the crack tip ($\alpha = 65^\circ$).

Fig 8: Dislocation density with and without gas bubble.

Fig 9: Plastic zone for two symmetric dislocation lines with and without gas bubble.

Fig 10: plastic zone with the number of gas bubbles.



Accession For	
NOIS GRA&I	
ERIC TAB	
Unannounced	
Identify for	
By	
Distribution	
Availability	
Dist	

At

Abstract.

During the loading of a crack edge dislocations are emitted from the crack tip forming a plastic zone. The presence of gas bubbles near the crack tip can change the plastic zone size and location drastically. A detailed study of the force field on an edge dislocation due to the crack load and gas bubbles allows for the determination of the plastic zone as a function of the inclination angle. The dislocation distribution along the plastic zone is found from force equilibrium considerations. Due to the presence of gas bubbles a shrinking and repulsion of the plastic zone from the crack tip is noticed. This process indicates the material embrittlement. The dislocation free zone (DFZ) near the crack tip grows. This embrittlement can become crucial in material design for fusion applications.

*Keywords: crack tip (fracturing);
Strength (mechanical); stress intensity;
dislocation; plastic zone; stress field;
tensile stress; Fusion reactions;
Nuclear reactions.*

Introduction.

The degradation of the inner walls of fusion reactors is a serious problem. The bombarding particles cause nuclear reactions which may produce considerable concentration of foreign elements inside the material (Ullmaier 1984). Here we concentrate on the (n,α) reactions which generate helium gas within the metals. Because of the low diffusion rate the helium basically stays where it is formed and can exert there a considerable pressure (Haubold 1983 and Jaeger et al. 1983).

In this article we study the influence of this bubble formation on the embrittlement of the material. Experiments have shown that plastic zones are formed during crack propagation due to the emission of dislocations. Several investigators have discussed the pile-up of screw dislocations in thin regions near the crack tip forming a plastic zone (Chang et al. 1981 and 1984). Here we develop a plasticity model for the thicker areas. Observations by means of the electron microscope have shown that edge dislocations are emitted occupying regions within angles 45 to 90 ° to the crack plane causing a zigzag propagation of the crack (Horton et al. 1982). Our model is able to point out to the location and the size of the plastic zone for different angles of inclination.

Employing the present model we would like to explain the so-called embrittlement in materials containing helium gas. Since all materials contain microcracks, under external loads dislocations are emitted from the crack tip and plastic zones are

formed. Our model shows that the presence of helium bubbles reduces the plastic zone size. This we believe is one of the prominent mechanisms underlying the process of embrittlement.

Stress Field in a plate with a line crack, under a pressure source.

In order to determine the force field on an edge dislocation due to a gas bubble in the neighbourhood of a crack, we need to know the stress field. To solve this problem we use the superposition principle. Consider a line crack $|x| < c, y = z = 0$, located in the plane $z = 0$ of rectangular coordinates (x, y, z) and a gas bubble at a point (ξ, η) outside the crack, fig 1. The pressure of the gas bubble will generate stresses on the crack surfaces. To free the crack surfaces from tractions we superpose the negative of the tractions induced by the bubble on the crack surfaces. The effect of the stress induced on the surface of the gas bubble due to this superposition is in the neighborhood of 0.1 % of the effect of the original bubble pressure for the configuration studied. Hence we will neglect this effect.

The total stress field is given by:

$$\sigma_{kl}^t(x, y) = \sigma_{kl}^b(x, y) + \sigma_{kl}^{bc}(x, y) \quad k, l = x, y \quad (1)$$

where

$\sigma_{ki}^t(x, y)$: total stress field

$\sigma_{ki}^b(x, y)$: stress field due to the gas bubble

$\sigma_{ki}^{bc}(x, y)$: stress field due to the interaction of the gas bubble with the crack.

It is important to note that the assumption of stress-free crack surfaces is only valid if the crack opens up, i.e. if the gas bubble generates tension along the crack.

For a gas bubble located at the origin of the coordinates, the normal stress σ_{yy} is given by (Eringen 1980):

$$\sigma_{yy} = a^2 p \frac{x^2 - y^2}{(x^2 + y^2)^2} \quad (2)$$

where a is the bubble radius and p is the bubble pressure. In order to generate a tensile load on the crack surface the bubble must be confined to a region of $\pm 45^\circ$ from the line of the crack, at the crack tip (fig 2).

We assume that the crack is symmetrically loaded, i.e. for a bubble situated at (ξ, η) there is a symmetrically situated bubble at $(-\xi, \eta)$ left of the y -axis. This results in a symmetric tensile stress and an antisymmetric shear stress. For our configurations the interaction between the two bubbles is negligible (Ling 1948).

In this way we split up the problem in two easily solved sub-units:

1. the stress due to a gas bubble is given by:

$$\sigma_{xx} = -a^2 p \frac{(x - \xi)^2 - (y - \eta)^2}{[(x - \xi)^2 + (y - \eta)^2]^2} \quad (3)$$

$$\sigma_{yy} = -\sigma_{xx} \quad (4)$$

$$\sigma_{xy} = -2a^2 p \frac{(x - \xi)(y - \eta)}{[(x - \xi)^2 + (y - \eta)^2]^2} \quad (5)$$

2. The calculation of the stress field due to an arbitrary symmetrically loaded crack reduces to a superposition of a symmetric mode-I problem and an antisymmetric mode-II problem.

The Boundary Conditions (B.C.) of the symmetric mode I problem are:

$$\sigma_{xy}|_{y=0} = 0 \quad (6)$$

$$\sigma_{yy}|_{\text{crack}} = -p(x) \quad (7)$$

$$u_y|_{\text{outside crack}} = 0 \quad (8)$$

$$p(x) = p(-x) \quad (9)$$

where σ_{kl} , ($k, l = x, y$) denote the stress tensor, (u_x, u_y) the displacement vector and $p(x)$ is the traction applied to the crack surface.

The stress field for this problem is given by (Sneddon et al. 1969, p 26):

$$\sigma_{xx}(x, y) = \sqrt{\frac{2}{\pi}} \int_0^\infty (y\xi - 1)\xi\psi(\xi)e^{-\xi y} \cos(\xi x) d\xi \quad (10)$$

$$\sigma_{yy}(x, y) = -\sqrt{\frac{2}{\pi}} \int_0^\infty (y\xi + 1)\xi\psi(\xi)e^{-\xi y} \cos(\xi x) d\xi \quad (11)$$

$$\sigma_{xy}(x, y) = -y \sqrt{\frac{2}{\pi}} \int_0^{\infty} \xi^2 \psi(\xi) e^{-\xi y} \sin(\xi x) d\xi \quad (12)$$

$$\sigma_{zz}(x, y) = \nu(\sigma_{xx} + \sigma_{yy}) \quad (13)$$

where

$$\psi(\xi) = \sqrt{\frac{\pi}{2}} \int_0^1 f(t) J_0(\xi t) dt \quad (14)$$

$$f(t) = \frac{2\pi}{\pi} \int_0^1 \frac{p(u) du}{\sqrt{t^2 - u^2}} \quad (15)$$

Here $J_n(z)$ denotes the Bessel's function of the first kind of order n .

The B.C. of the antisymmetric mode II problem are:

$$\sigma_{yy}|_{y=0} = 0 \quad (16)$$

$$\sigma_{xy}|_{\text{crack}} = -q(x) \quad (17)$$

$$u_x|_{\text{outside crack}} = 0 \quad (18)$$

$$q(x) = -q(-x) \quad (19)$$

where $q(x)$ is the shear stress applied to the crack surface.

The solution of this problem is:

$$\sigma_{xx}(x, y) = -\sqrt{\frac{2}{\pi}} \int_0^{\infty} (\xi y - 2) \xi \psi(\xi) e^{-\xi y} \cos(\xi x) d\xi \quad (20)$$

$$\sigma_{yy}(x, y) = \sqrt{\frac{2}{\pi}} \int_0^{\infty} \xi^2 y \psi(\xi) e^{-\xi y} \cos(\xi x) d\xi \quad (21)$$

$$\sigma_{xy}(x, y) = \sqrt{\frac{2}{\pi}} \int_0^{\infty} (\xi y - 1) \xi \psi(\xi) e^{-\xi y} \sin(\xi x) d\xi \quad (22)$$

$$\sigma_{zz}(x, y) = \nu(\sigma_{xx} + \sigma_{yy}) \quad (23)$$

where

$$\psi(\xi) = \sqrt{\frac{\pi}{2}} \int_0^1 f(t) J_1(\xi t) dt \quad (24)$$

$$f(t) = \frac{2}{\pi} \int_0^t \frac{uq(u) du}{\sqrt{t^2 - u^2}} \quad (25)$$

These solutions involve quite tedious triple integrations. By expanding $p(x)$ and $q(x)$ into Fourier series, we managed to reduce the triple integrations to single ones, resulting in the following solutions:

Symmetric mode-I:

$$p(x) = \sum_{n=0}^{\infty} p_n \cos(n\pi x) \quad (26)$$

$$\sigma_{kl} = \sum_{n=0}^{\infty} p_n \sigma_{kl}^n(x, y) \quad (k, l = x, y) \quad (27)$$

where

$$\sigma_{xx}^n(x, y) = \int_0^1 \mathcal{U}_0(n\pi t) [yh(x, y, t) - f(x, y, t)] dt \quad (28)$$

$$\sigma_{yy}^n(x, y) = - \int_0^1 \mathcal{U}_0(n\pi t) [f(x, y, t) + yh(x, y, t)] dt \quad (29)$$

$$\sigma_{xy}^n(x, y) = -y \int_0^1 \mathcal{U}_0(n\pi t) j(x, y, t) dt \quad (30)$$

Antisymmetric mode-II:

$$q(x) = \sum_{n=1}^{\infty} q_n \sin(n\pi x) + q_0 x \quad (31)$$

$$\sigma_{ki} = \sum_{n=0}^{\infty} q_n \sigma_{ki}^n(x, y) \quad (k, l = x, y) \quad (32)$$

where

$$\sigma_{xx}^n(x, y) = - \int_0^1 g_n(t) [yh^*(x, y, t) - 2f^*(x, y, t)] dt \quad (33)$$

$$\sigma_{yy}^n(x, y) = y \int_0^1 g_n(t) h^*(x, y, t) dt \quad (34)$$

$$\sigma_{xy}^n(x, y) = \int_0^1 g_n(t) [yh_s(x, y, t) - f_s(x, y, t)] dt \quad (35)$$

$$g_n(t) = \mathcal{U}_1(n\pi t) \quad n \geq 1 \quad (36)$$

$$g_0(t) = t^2 / 2 \quad (37)$$

The term $q_0 x$ in (31) is to account for a non zero shear stress at the crack tip.

The functions $f(x, y, t)$, $h(x, y, t)$, $j(x, y, t)$, $f^*(x, y, t)$, $h^*(x, y, t)$, $f_s(x, y, t)$ and $h_s(x, y, t)$ are collected in the appendix.

Along the crack line a great deal of simplifications are achieved:

Symmetric mode-I

$$\sigma_{xx}^n(x, 0) = x \int_0^1 \frac{tJ_0(n\pi t)dt}{(x^2 - t^2)^{3/2}} \quad (38)$$

$$\sigma_{yy}^n(x, 0) = \sigma_{xx}^n(x, 0) \quad (39)$$

$$\sigma_{xy}^n(x, 0) = 0 \quad (40)$$

Antisymmetric mode-II

$$\sigma_{xx}^n(x, 0) = 0 \quad (41)$$

$$\sigma_{yy}^n(x, 0) = 0 \quad (42)$$

$$\sigma_{xy}^n(x, 0) = \int_0^1 \frac{tf(t)dt}{(x^2 - t^2)^{3/2}} \quad (43)$$

where

$$g_n(t) = tJ_1(n\pi t) \quad n \geq 1 \quad (44)$$

$$g_0(t) = t^2/2 \quad (45)$$

Hence we have the solution of a rather general problem in a form attractive to computations. The generality will allow us later on to take into account the influence of any kind of in-plane defects on the plastic zone size and position.

Method of approach.

Experimental observations indicate that from the crack tip emanate one, or two sets of edge dislocations making an average angle $\pm\alpha$ with the crack line. We idealize this picture by assuming that the edge dislocations constitute two straight lines.

ζ and t are local coordinates along the plastic zone ($t, \zeta \in [0, L]$), fig 1. ζ_2, ζ_3 and ζ_4 are symmetrically located points with respect to ζ : if ζ corresponds to (x, y) , then ζ_2 corresponds to $(-x, y)$, ζ_3 to $(-x, -y)$ and ζ_4 to $(x, -y)$.

At first we look at the case of just one set of dislocations (fig 3) at each crack tip.

We distinguish five kinds of forces on any of these dislocations:

1. The force \vec{F}_e due to all 'external' sources, i.e sources not linked to the dislocations generated.

$$\vec{F}_e(t) = b(t)\vec{F}_0(t) \quad (46)$$

where $b(t)$ is the Burger's vector density at t ,

$$\begin{aligned} \vec{F}_0(t) = & \left\{ \left[\sigma_{xy}^e(t) \cos(\alpha) + \sigma_{yy}^e(t) \sin(\alpha) \right] \vec{e}_x \right. \\ & \left. - \left[\sigma_{xx}^e(t) \cos(\alpha) + \sigma_{xy}^e(t) \sin(\alpha) \right] \vec{e}_y \right\} \end{aligned} \quad (47)$$

$\sigma_{kl}^e(t)$ ($k, l = x, y$) is the 'external' stress field at t .

In the case under investigation we have:

$$\sigma_{kl}^e(t) = \sigma_{kl}^c(t) + \sigma_{kl}^b(t) + \sigma_{kl}^{bc}(t) \quad (48)$$

and hence σ_{kl}^e consists of three contributions:

$\sigma_{kl}^c(t)$: the stress field due to the external crack loading.

$\sigma_{kl}^b(t)$: the stress field due to the gas bubbles.

$\sigma_{kl}^{bc}(t)$: the stress field due to the interaction of the gas bubbles with the crack.

2. The force \vec{F}_d due to the other dislocations in zone 1.

$$\vec{F}_d(t) = b(t) \int_0^L \vec{K}_1(t, \zeta) b(\zeta) d\zeta \quad (49)$$

where

$$\vec{K}_1(t, \zeta) = \frac{\mu}{2\pi(1-\nu)(t-\zeta)} \vec{e}_1 \quad (50)$$

Here μ is the shear modulus and ν is Poisson's ratio.

3. The force \vec{F}_{ds} due to the y-symmetrically located dislocations.

$$\vec{F}_{ds}(t) = b(t) \int_0^L b(\zeta) \vec{K}_2(t, \zeta) d\zeta \quad (51)$$

where

$$\begin{aligned} \vec{K}_2(t, \zeta) = & \left\{ \left[\sigma_{xy}^{ds}(t, \zeta) \cos(\alpha) + \sigma_{yy}^{ds}(t, \zeta) \sin(\alpha) \right] \vec{e}_x \right. \\ & \left. - \left[\sigma_{xx}^{ds}(t, \zeta) \cos(\alpha) + \sigma_{xy}^{ds}(t, \zeta) \sin(\alpha) \right] \vec{e}_y \right\} \end{aligned} \quad (52)$$

$\sigma_{ki}^{ds}(t, \zeta)$ is the stress field at t due to a unit Dirac-delta dislocation density at ζ_2 .

4. The force \vec{F}_{cd} due to the interaction of all dislocations with the crack.

$$\vec{F}_{cd}(t) = b(t) \int_0^L b(\zeta) \vec{K}_3(t, \zeta) d\zeta \quad (53)$$

where

$$\begin{aligned} \vec{K}_3(t, \zeta) = & \left\{ \left[\sigma_{xy}^{cd}(t, \zeta) \cos(\alpha) + \sigma_{yy}^{cd}(t, \zeta) \sin(\alpha) \right] \vec{e}_x \right. \\ & \left. - \left[\sigma_{xx}^{cd}(t, \zeta) \cos(\alpha) + \sigma_{xy}^{cd}(t, \zeta) \sin(\alpha) \right] \vec{e}_y \right\} \end{aligned} \quad (54)$$

$\sigma_{ki}^{cd}(t, \zeta)$ is the stress field at t due to the interaction of the crack with a unit Dirac-delta dislocation density at ζ and at ζ_2 .

5. The force \vec{F}_f due to friction in the glide plane of the dislocation.

$$\vec{F}_f(t) = -c_f b(t) \vec{e}_t \quad (55)$$

where c_f is of the order of

$$c_f = 10^{-4} \mu \text{ a } 10^{-2} \mu \quad (56)$$

The equilibrium configuration of the system requires that:

$$\vec{F}_e + \vec{F}_d + \vec{F}_{ds} + \vec{F}_{cd} + \vec{F}_f = 0 \quad (57)$$

or

$$\vec{F}_0(t) + \int_0^L [\vec{K}_1(t, \zeta) + \vec{K}_2(t, \zeta) + \vec{K}_3(t, \zeta)] b(\zeta) d\zeta - c_f \vec{e}_t = 0 \quad (58)$$

At first we neglect the interaction forces \vec{F}_{ds} and \vec{F}_{cd} . Hence we have:

$$\vec{F}_0(t) + \int_0^L \vec{K}_1(t, \zeta) b(\zeta) d\zeta - c_f \vec{e}_t = 0 \quad (59)$$

Due to the chosen configuration the forces between the dislocations \vec{F}_d are parallel to their line of position, i.e. they have the same angle of inclination. Indeed, substituting (50) in (59) one obtains:

$$\vec{F}_0(t) + \vec{e}_t \left[\int_0^L K_1(t, \zeta) b(\zeta) d\zeta - c_f \right] = 0 \quad (60)$$

where

$$K_1(t, \zeta) = |\vec{K}_1(t, \zeta)| \quad (61)$$

Hence, in order to maintain the equilibrium the forces due to the crack load must also have an inclination angle α (a necessary condition). From this we deduce the following approach to the solution of our problem:

- i. We choose an angle α .
- ii. We determine the force field \vec{F}_0 due to the crack load on an edge dislocation with this angle of inclination.
- iii. In this force field we look for a straight line with inclination angle α , of forces having this same inclination angle. This gives us the size and position of the plastic zone.
- iv. Knowing the force field along this line, we can calculate the edge dislocation distribution (Burger's vector) which will generate a force field with the opposite sign (force equilibrium). This requires the solution of the following integral equation:

$$\int_0^L K_1(t, \zeta) b(\zeta) d\zeta = -f(t) \quad (62)$$

where

$$f(t) = F_0(t) - c_f \quad (63)$$

$$F_0(t) = |\vec{F}_0(t)| \quad (64)$$

- v. The interaction forces between crack and dislocations can be treated by iteration. Let the solution of (62) be $b_0(t)$. The dislocation density $b_1(t)$, after one iteration is given by the solution of

$$\vec{F}_0(t) + \int_0^L \vec{K}_1(t, \zeta) b_1(\zeta) d\zeta + \int_0^L [\vec{K}_2(t, \zeta) + \vec{K}_3(t, \zeta)] b_0(\zeta) d\zeta - c_f \vec{e}_t = 0 \quad (65)$$

The iterated location of the plastic zone is determined by the force field

$$\vec{F}_1(t) = \vec{F}_0(t) + \int_0^L [\vec{K}_2(t, \zeta) + \vec{K}_3(t, \zeta)] b_0(\zeta) d\zeta \quad (66)$$

and the density $b_1(t)$ is the solution of

$$\int_0^L K_1(t, \zeta) b_1(\zeta) d\zeta = -f_1(t) \quad (67)$$

where

$$f_1(t) = |\vec{F}_1| - c_f \quad (68)$$

In case of two symmetrically located dislocation lines (fig 4), our equations do not change on condition that we redefine σ_{ki}^{ds} and σ_{ki}^{cd} :

$\sigma_{ki}^{ds}(t, \zeta)$ is the stress field at t due to a unit Dirac-delta dislocation density at ζ_2 , ζ_3 and ζ_4 , i.e. all x - and y - symmetric positions of $t = \zeta$.

$\sigma_{ki}^{cd}(t, \zeta)$ is the stress field at t due to the interaction of the crack with a unit Dirac-delta dislocation density at $t = \zeta$ and all its x - and y -symmetric positions.

Due to the significance of the correction forces, iteration is more important in the symmetric case.

The determination of the edge dislocation distribution corresponding to the calculated force field amounts to the solution of the following Cauchy integral equation for $b(x)$ (62):

$$\int_0^L \frac{b(\zeta) \mu d\zeta}{2\pi(1-\nu)(\zeta-t)} = f(t) \quad (69)$$

or

$$\int_0^L \frac{\varphi(\zeta) d\zeta}{\zeta - t} = f(t) \quad 0 \leq t \leq L \quad (70)$$

where

$$\varphi(\zeta) = \frac{\mu b(\zeta)}{2\pi(1-\nu)} \quad (71)$$

The solution of (70) which is zero at L is given by Mikhlin 1979 p 130:

$$\varphi(t) = \frac{1}{\pi^2 \sqrt{t(L-t)}} \left\{ \int_t^L \frac{[\zeta(L-\zeta)]^{1/2}}{t-\zeta} f(\zeta) d\zeta - \int_0^L \left[\frac{\zeta}{L-\zeta} \right]^{1/2} f(\zeta) d\zeta \right\} \quad (72)$$

$$t \in [0, L] \quad (73)$$

The first integral is a Cauchy integral whose singularity can be removed as follows:

we write the integral as one centered about the singularity and the rest: for $t \leq L/2$:

$$I = \int_0^L \frac{[\zeta(L-\zeta)]^{1/2}}{t-\zeta} f(\zeta) d\zeta = \int_{-1}^1 \frac{[\zeta(L-\zeta)]^{1/2}}{t-\zeta} f(\zeta) d\zeta = \int_{-1}^1 \frac{[\zeta(L-\zeta)]^{1/2}}{t-\zeta} f(\zeta) d\zeta + \int_{-1}^1 \frac{[\zeta(L-\zeta)]^{1/2}}{t-\zeta} f(\zeta) d\zeta \quad (74)$$

Then we subtract the constant contribution of the numerator of the first integral

which removes the singularity. In this way we obtain:

for $t \leq L/2$:

$$I = \int_{-1}^1 \left\{ [(t-u)(L-t+u)]^{1/2} f(t-u) - [t(L-t)]^{1/2} f(t) \right\} \frac{du}{u} \\ + \int_{-1}^1 \frac{[\zeta(L-\zeta)]^{1/2}}{t-\zeta} f(\zeta) d\zeta \quad (75)$$

for $t > L/2$:

$$I = \int_0^{2t-L} \frac{[\zeta(L-\zeta)]^{1/2}}{t-\zeta} f(\zeta) d\zeta \\ + \int_{t-1}^{1-t} \left\{ [(t-u)(L-t+u)]^{1/2} f(t-u) - [t(L-t)]^{1/2} f(t) \right\} \frac{du}{u} \quad (76)$$

Results and discussion.

The present model was applied to the study of helium embrittlement in fusion reactors. During the fusion process helium is being formed in the containing wall whose embrittlement could lead to serious structural problems. In our case study we lined up one or more helium bubbles in front of the tip of a typical microcrack and studied how this affected the location and extent of the plastic zone(s) around the tip.

In all of our calculations we kept the bubble radius, bubble pressure and crack load constant. For these quantities we took the following typical values (Haubold 1983 and Jaeger et al. 1983)

bubble radius $a = 0.68 \times 10^{-9} m$

bubble pressure $p_0 = 5 \times 10^{10} N m^{-2}$

crack load $\sigma_c = 3 \times 10^8 N m^{-2}$

First we considered only one gas bubble at a distance d from the crack tip and assumed that only one plastic zone is formed: n (number of plastic zones) = 1. To keep a maximum accuracy for a minimum number of terms in our Fourier expansion we set the crack length c equal to d . This makes the relative distance of the gas bubble from the crack tip unity.

Figs 5, 6 and 7 display the plastic zones for $\alpha = 55^\circ, 60^\circ$ and 65° for different values of d . From these we see that the closer the gas bubble to the crack tip the more the plastic zone shrinks and moves away from the tip. This agrees with the global notion of embrittlement which can be understood as a reduction of the plastic zone. Fig 8 shows the dislocation distribution with and without bubble for the normalized plastic zone. They look quite similar and generally the distribution itself is not much influenced.

So far we have considered only one dislocation pileup. The case of two symmetrically placed distributions is depicted in fig 9. Here several iterations were performed. The results point in the same direction, namely, the presence of the gas bubble removes and reduces the plastic zone.

Finally the case of several equidistant gas bubbles lined up in front of the crack tip is shown in fig 10. The interaction between the gas bubbles is negligible for

our configuration (Ling 1948). While an increase in the number of gas bubbles intensifies the embrittlement effect, the impact of each individual gas bubble decreases fast as a function of its distance from the tip.

Hence we can conclude that the presence of one or more gas bubbles in front of the crack tip reduces and removes the plastic zone. This results in a more brittle behaviour of the material around the crack tip and can eventually lead to a brittle fracture.

Summary.

The present analysis has indicated that the presence of one or more gas bubbles in front of a crack removes and decreases the plastic zone around the crack tip. This leads to an embrittlement of the material and ultimately brittle fracture. The distance of the gas bubble to the crack tip is a major parameter in this phenomenon.

Acknowledgement

The authors express their appreciation to Professor R.G. Mills for the encouragement and support received.

Appendix

We can express $f(x, y, t)$, $h(x, y, t)$, $j(x, y, t)$, $f^{\bullet}(x, y, t)$, $h^{\bullet}(x, y, t)$, $h_s(x, y, t)$ and $f_s(x, y, t)$ as a function of three other functions $H_1(p)$, $H_2(p, q)$ and $H_3(x, y, t)$:

$$f(x, y, t) = -H_1(y) \quad (77)$$

$$h(x, y, t) = H_2(y, y) \quad (78)$$

$$j(x, y, t) = H_2(x, y) \quad (79)$$

$$f^{\bullet}(x, y, t) = -H_1(t) \quad (80)$$

$$h^{\bullet}(x, y, t) = H_2(y, t) \quad (81)$$

$$h_s(x, y, t) = H_2(x, t) \quad (82)$$

$$f_s(x, y, t) = H_3(x, y, t) \quad (83)$$

where

$$H_1(p) = \frac{-1}{2\sqrt{j}} (\mathcal{E}_1^{-1/2} + \mathcal{E}_2 \mathcal{E}_1^{-1})^{-1/2} \left[-\frac{1}{2} \mathcal{E}_1^{-3/2} \mathcal{E}_{1p} + \mathcal{E}_{2p} \mathcal{E}_1 - \mathcal{E}_{1p} \mathcal{E}_2 \mathcal{E}_1^{-2} \right] \quad (84)$$

$$\begin{aligned}
H_2(p, q) &= \frac{-1}{4\sqrt{2}} (\mathfrak{E}_1^{-1,2} + \mathfrak{E}_2 \mathfrak{E}_1^{-1})^{-3,2} \left[-\frac{1}{2} \mathfrak{E}_1^{-3,2} \mathfrak{E}_{1p} + \mathfrak{E}_{2p} \mathfrak{E}_1 - \mathfrak{E}_{1p} \mathfrak{E}_2 \mathfrak{E}_1^{-2} \right] x \\
&+ x \left[-\frac{1}{2} \mathfrak{E}_1^{-3,2} \mathfrak{E}_{1q} + \mathfrak{E}_{2q} \mathfrak{E}_1 - \mathfrak{E}_{1q} \mathfrak{E}_2 \mathfrak{E}_1^{-2} \right] + \frac{1}{2\sqrt{2}} (\mathfrak{E}_1^{-1,2} + \mathfrak{E}_2 \mathfrak{E}_1^{-1})^{-1,2} x \\
&+ x \left\{ -\frac{1}{2} \mathfrak{E}_1^{-3,2} \mathfrak{E}_{1pq} + (\mathfrak{E}_{2pq} \mathfrak{E}_1 + \mathfrak{E}_{2p} \mathfrak{E}_{1q} - \mathfrak{E}_{1pq} \mathfrak{E}_2 - \mathfrak{E}_{1p} \mathfrak{E}_{2q}) \mathfrak{E}_1^{-2} + \right. \\
&\left. + \frac{3}{4} \mathfrak{E}_1^{-5,2} \mathfrak{E}_{1q} \mathfrak{E}_{1p} - (\mathfrak{E}_{2p} \mathfrak{E}_1 - \mathfrak{E}_{1p} \mathfrak{E}_2) 2 \mathfrak{E}_{1q} \mathfrak{E}_1^{-3} \right\}
\end{aligned} \tag{85}$$

$p, q = x, y$ or t

$$\begin{aligned}
H_3(x, y, t) &= \frac{-2x(\mathfrak{E}_{3iy} + \mathfrak{E}_{4iy})}{(\mathfrak{E}_3 + \mathfrak{E}_4)(\mathfrak{E}_3 + \mathfrak{E}_4)^2 - 4x^2} + \\
&+ \frac{2x(\mathfrak{E}_{3i} + \mathfrak{E}_{4i})}{(\mathfrak{E}_3 + \mathfrak{E}_4)^2 ((\mathfrak{E}_3 + \mathfrak{E}_4)^2 - 4x^2)} \left[(\mathfrak{E}_{3iy} + \mathfrak{E}_{4iy}) ((\mathfrak{E}_3 + \mathfrak{E}_4)^2 - 4x^2)^{1/2} + \right. \\
&\left. + (\mathfrak{E}_3 + \mathfrak{E}_4)^2 (\mathfrak{E}_{3y} + \mathfrak{E}_{4y}) ((\mathfrak{E}_3 + \mathfrak{E}_4)^2 - 4x^2)^{-1/2} \right]
\end{aligned} \tag{86}$$

in which:

$$\mathfrak{E}_1 = (y^2 + t^2 - x^2)^2 + 4x^2 y^2 \tag{87}$$

$$\mathfrak{E}_2 = y^2 + t^2 - x^2 \tag{88}$$

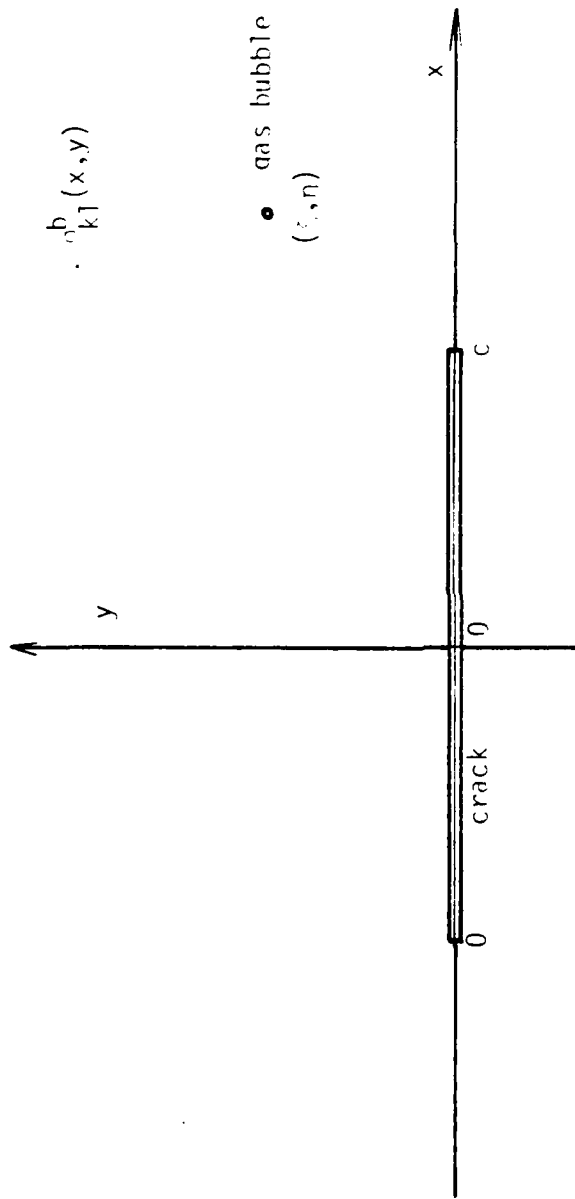
$$\mathfrak{E}_3 = [y^2 + (t + x)^2]^{1/2} \tag{89}$$

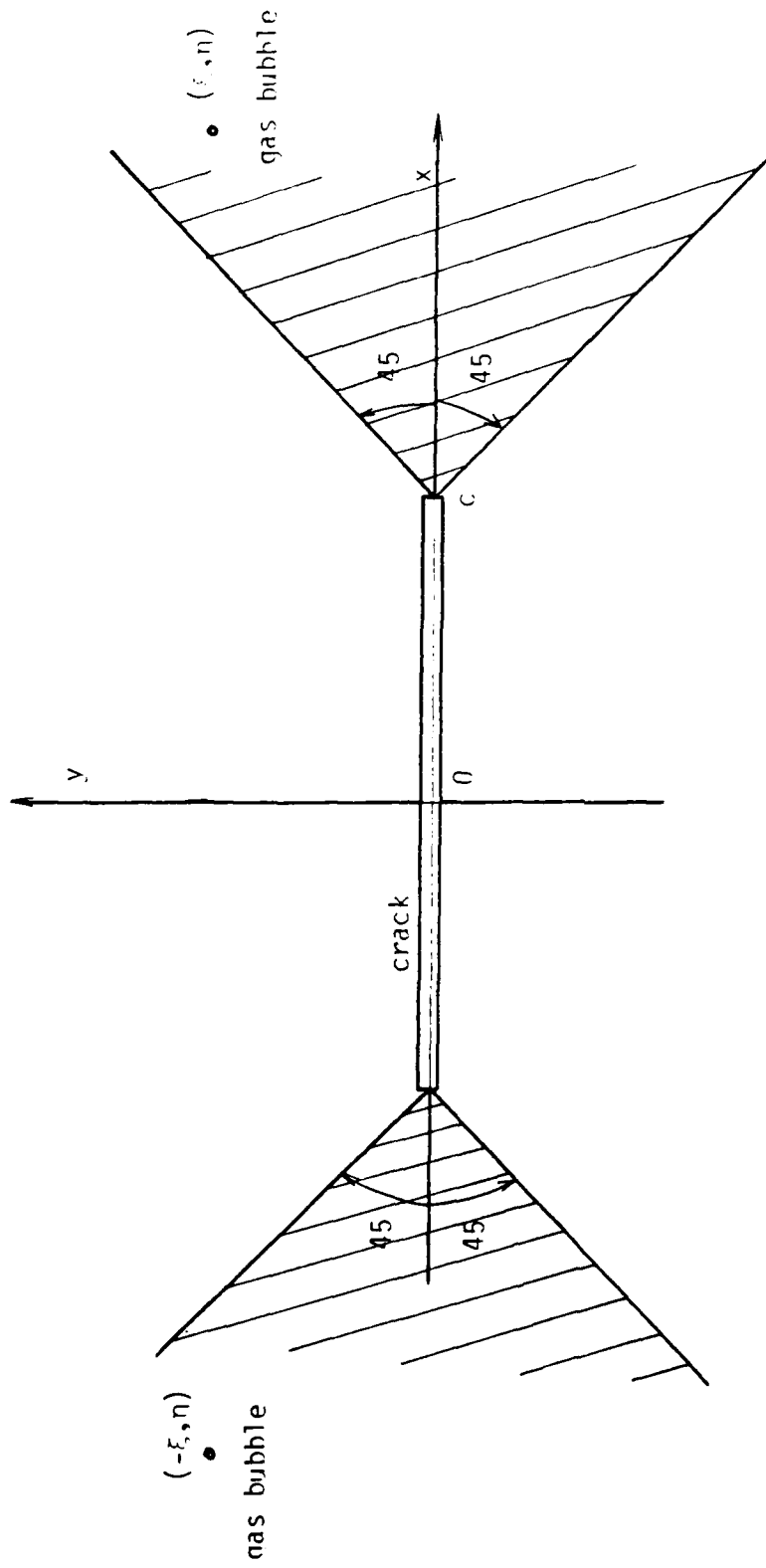
$$\mathfrak{E}_4 = [y^2 + (x - t)^2]^{1/2} \tag{90}$$

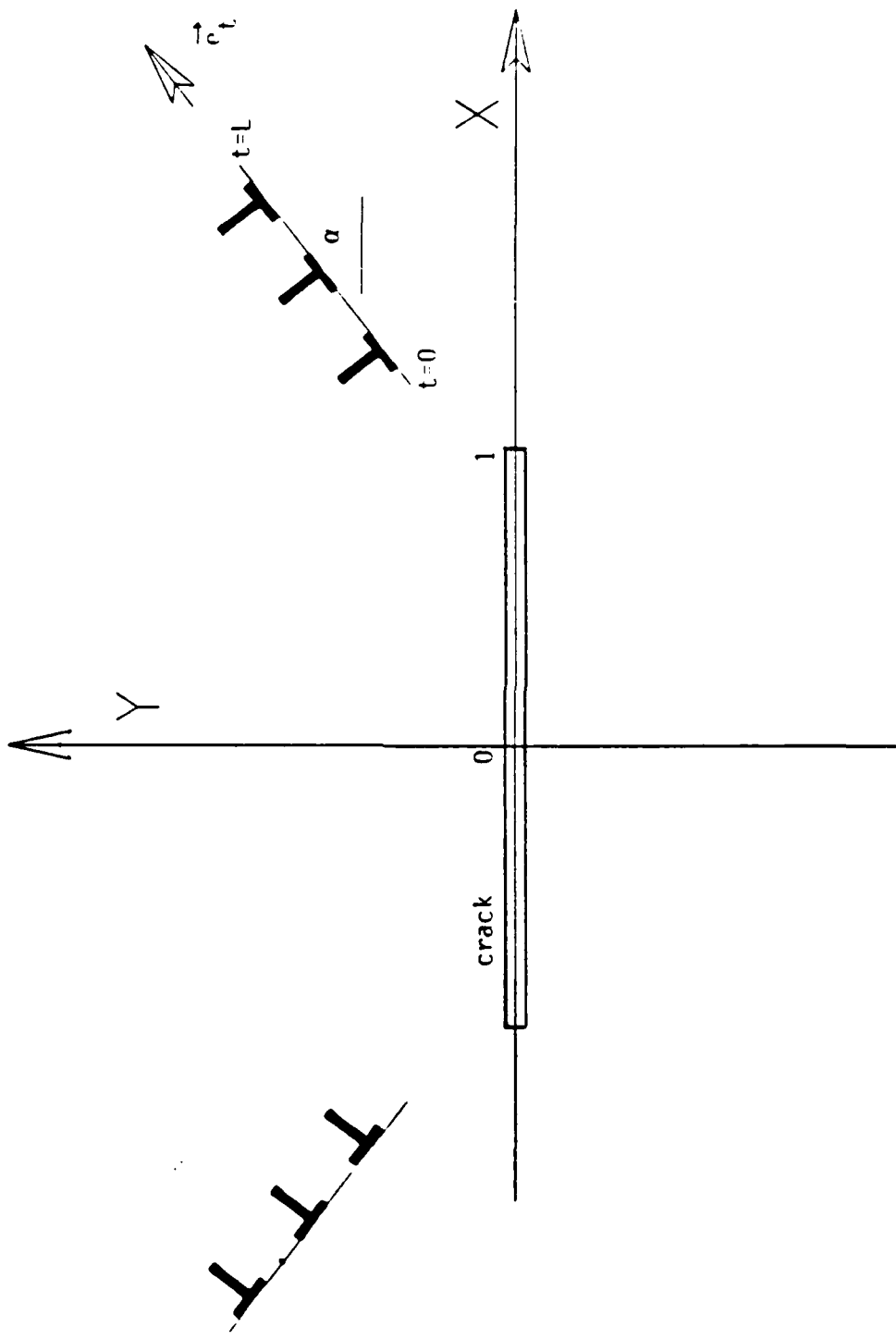
The subscripts x , y , t , p and q represent partial derivatives with respect to x , y , t , p , and q .

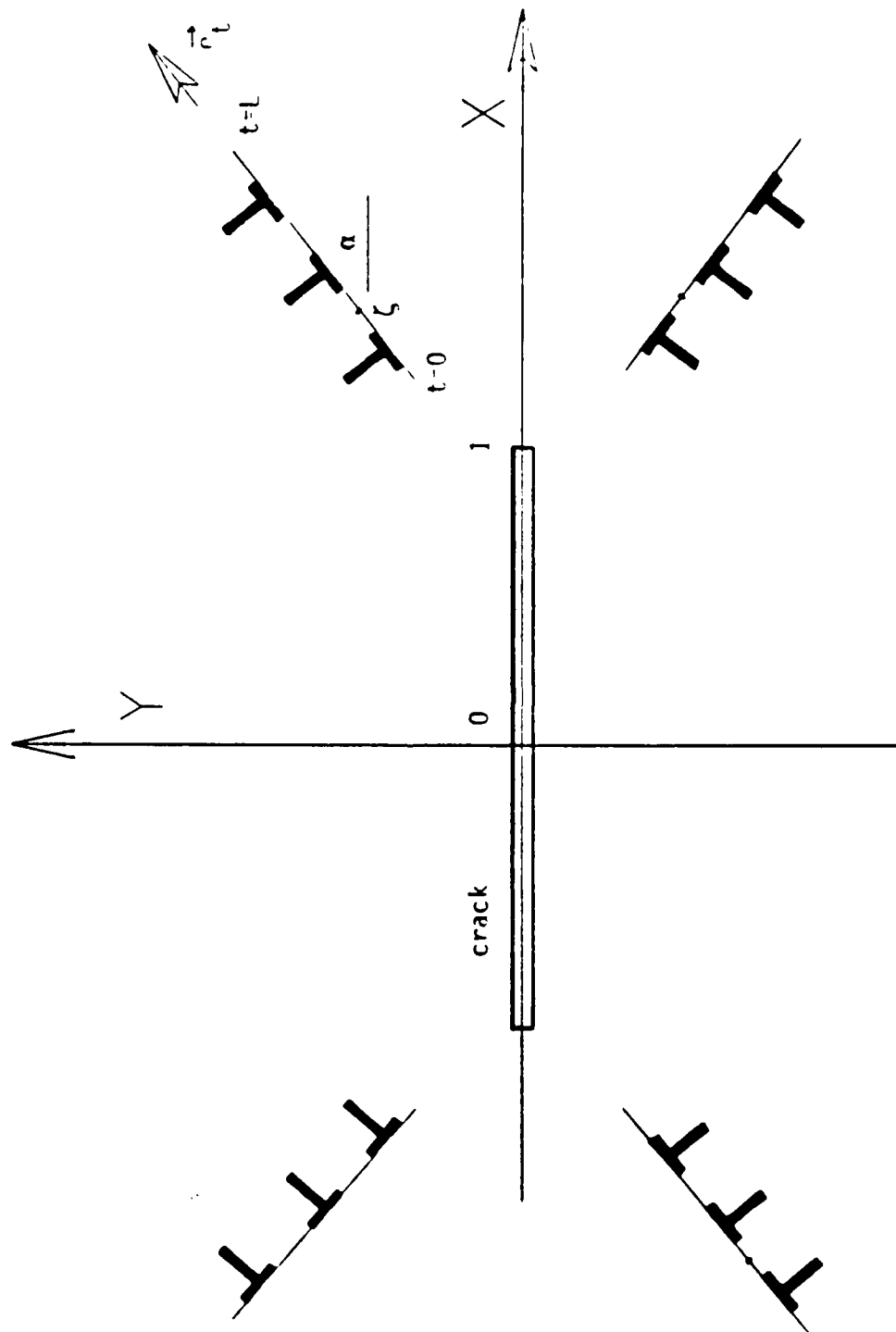
Bibliography

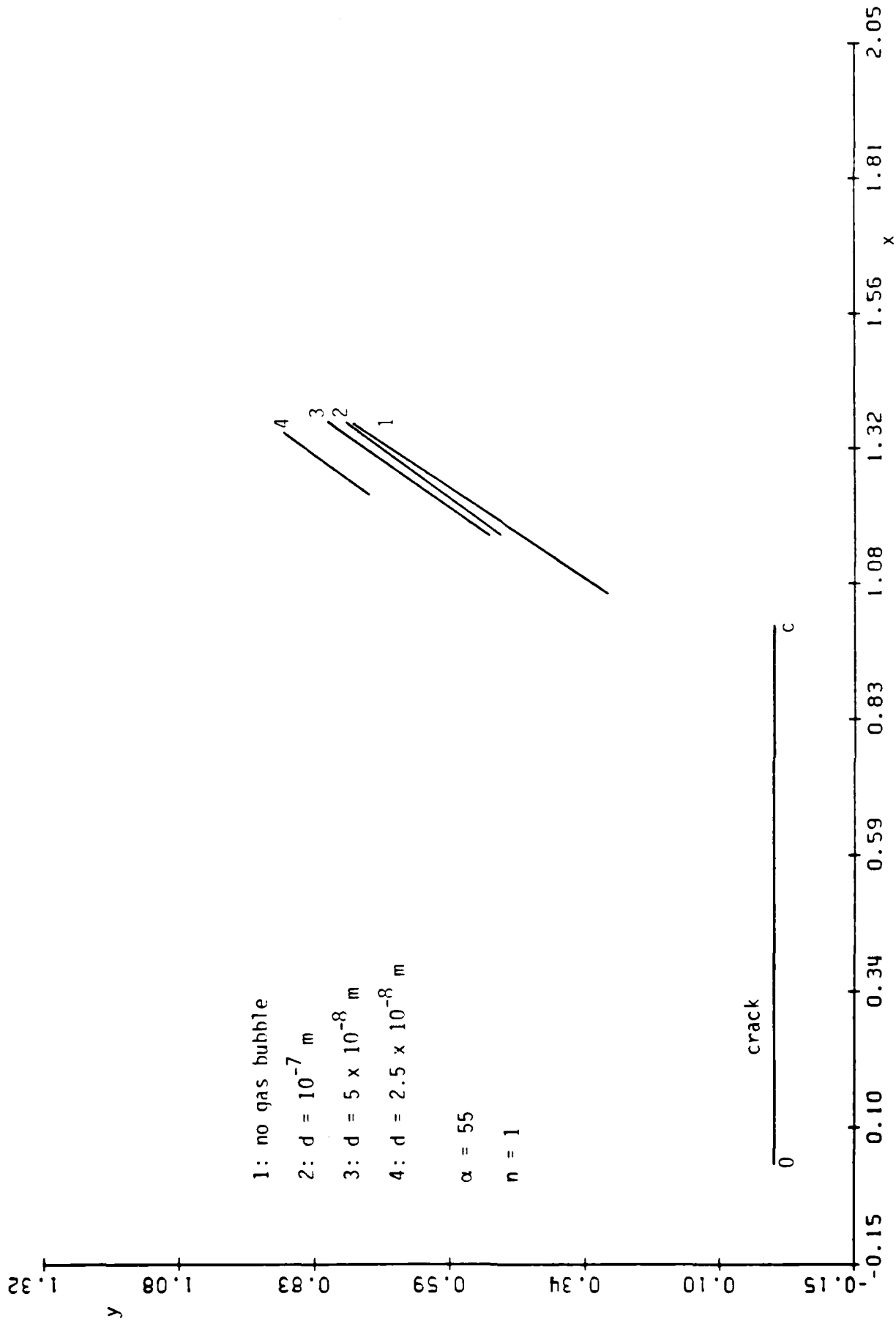
1. Chang, S.-J., and Ohr, S.M., *J.Appl.Phys.* **52** (1981) p. 7174.
2. Chang, S.-J., and Ohr, S.M., *J.Appl.Phys.* **55** (1984) p. 3505.
3. Eringen, A.C., *Mechanics of Solids*, Robert E. Krieger Publishing Company (1980).
4. Haubold, H.-G., *Radiation Effects* **78** (1983) p. 385.
5. Horton, J.A., and Ohr, S.M., *J.Mater.Sci.* **17** (1982) p. 3140.
6. Jaeger, W., Manzke, R., Trinkaus, H., Zeller, R., Fink, J., and Crecelius, G., *Radiation Effects* **78** (1983) p. 315.
7. Ling, Chih-Bing, *J. Appl. Phys.* **19** (1948) p. 77.
8. Mikhlin, S.G., *Integral Equations*, Macmillan Company (1979).
9. Sneddon, I.N., and Lowengrub, M., *Crack Problems in the Classical Theory of Elasticity*, John Wiley & Sons, Inc (1969).
10. Ullmaier, H., *Nuclear Fusion* **24** (1984) p. 1039.

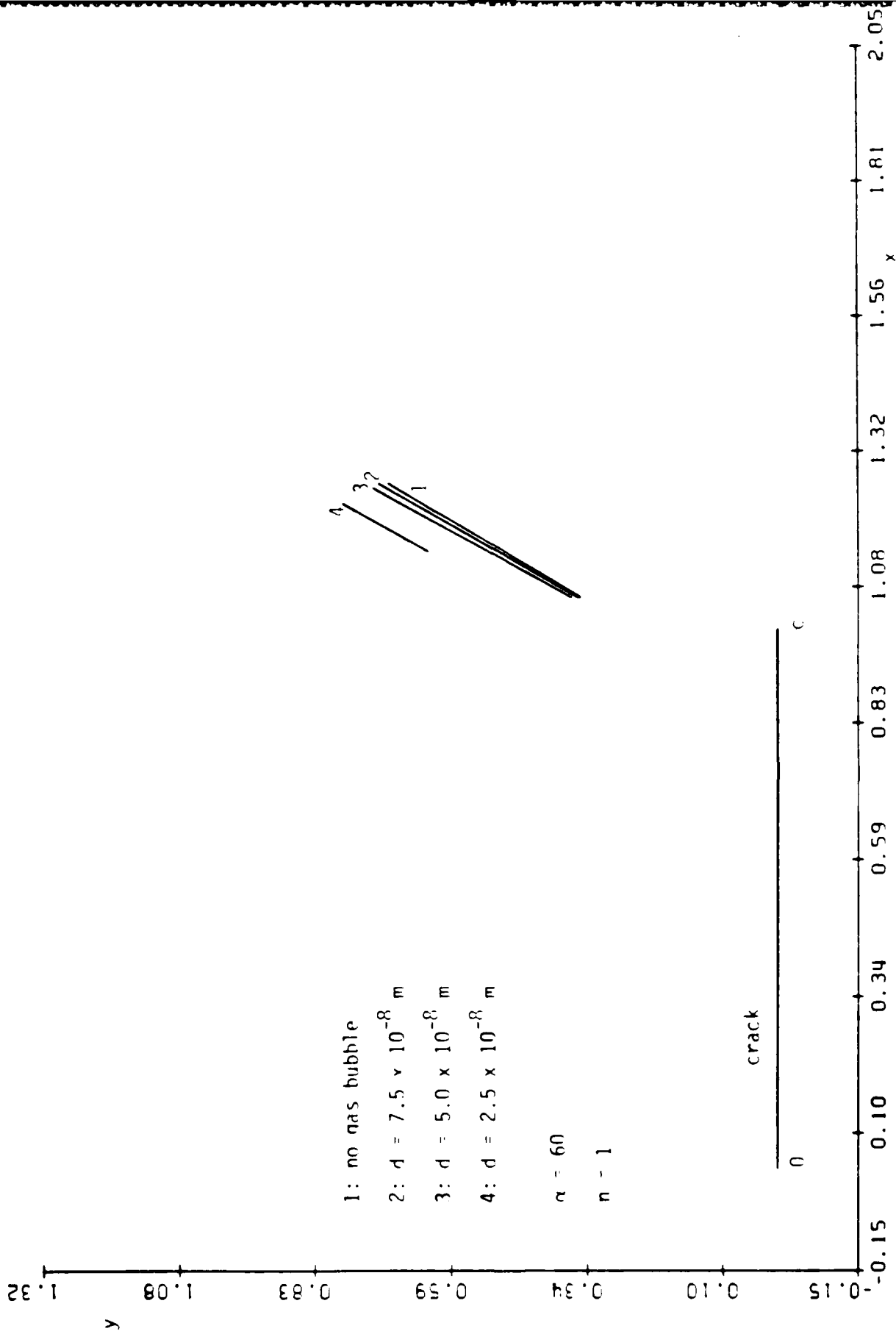


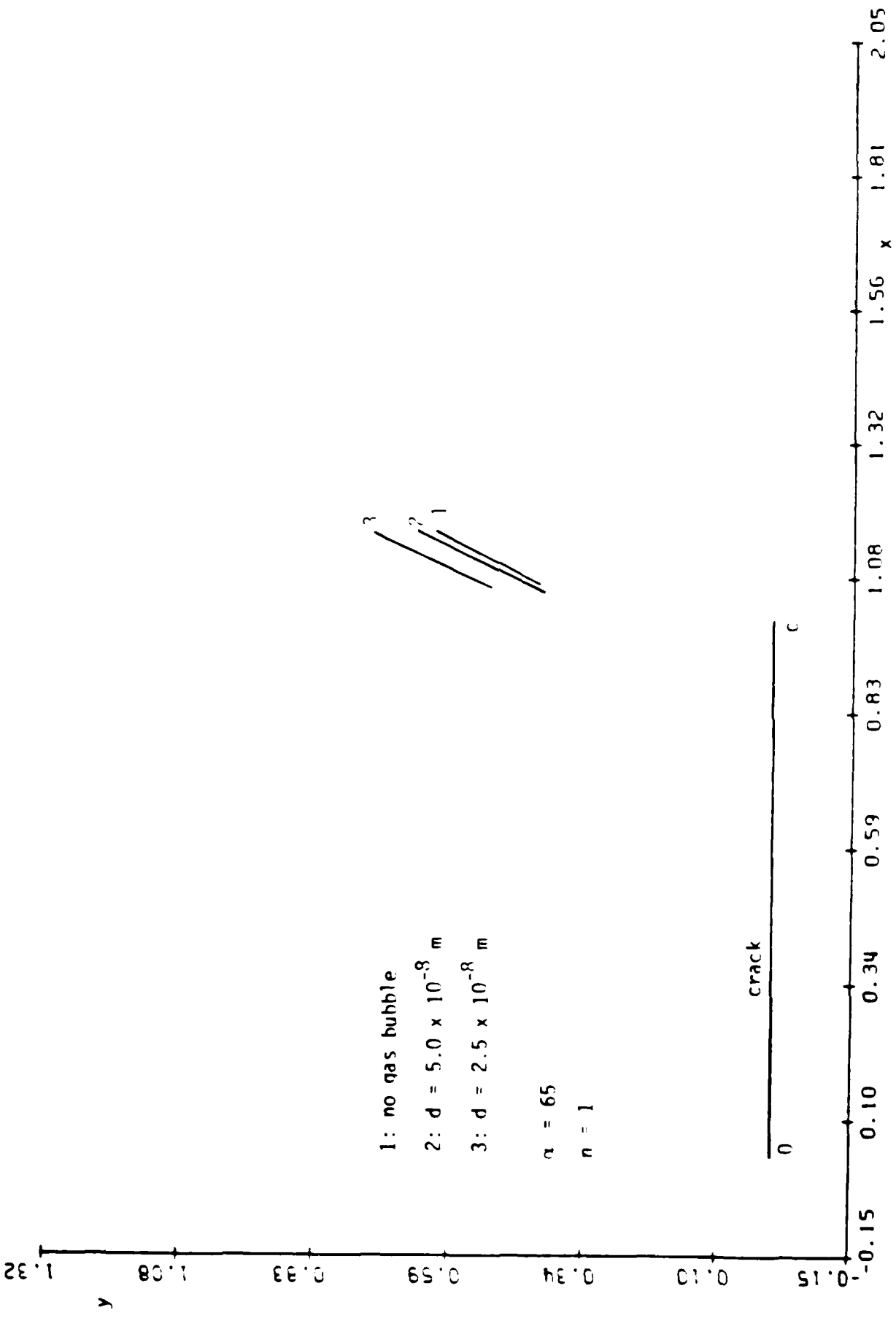












1: no gas bubble

2: $d = 5.0 \times 10^{-8}$ m

3: $d = 2.5 \times 10^{-8}$ m

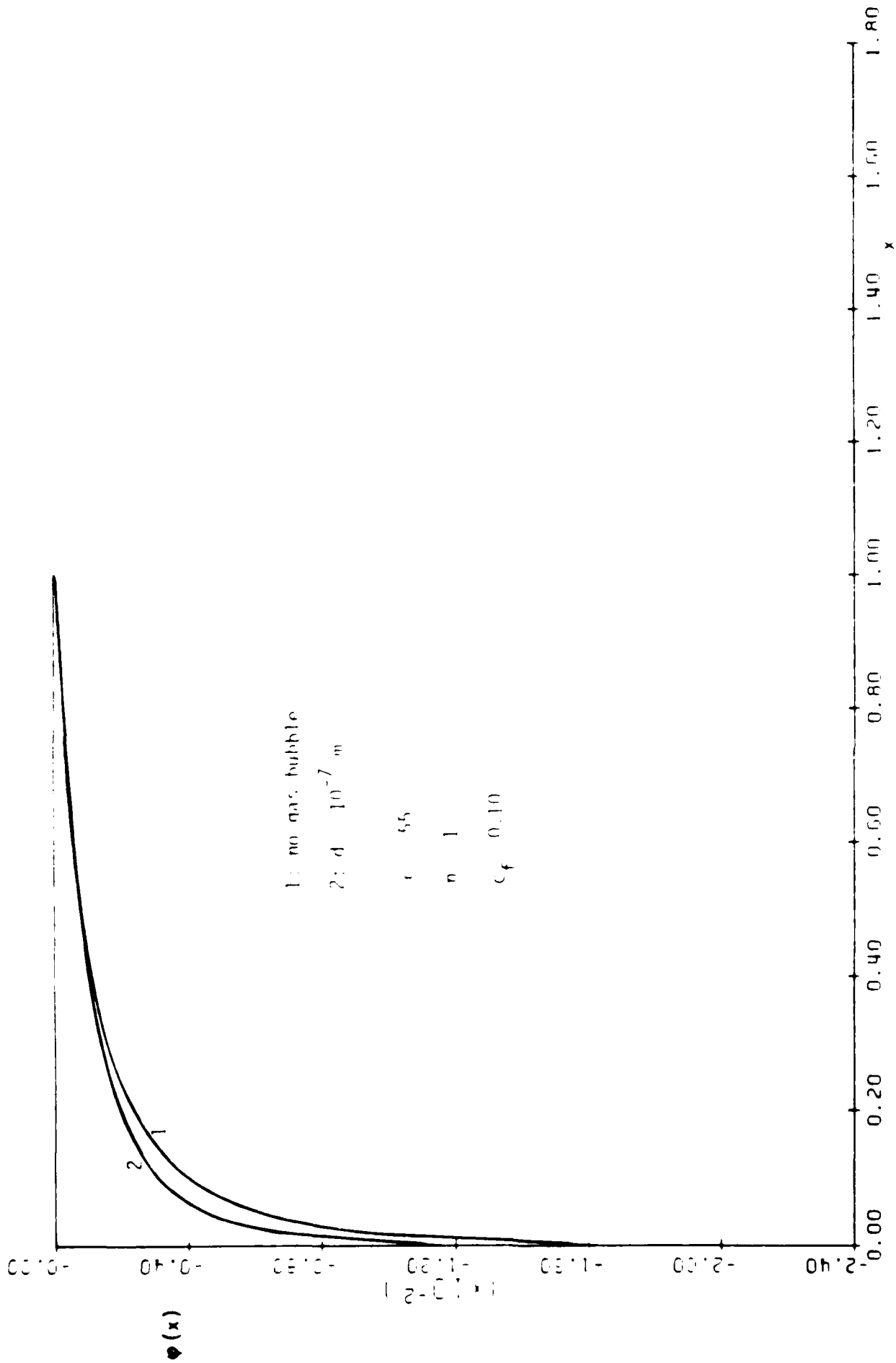
$\alpha = 65$

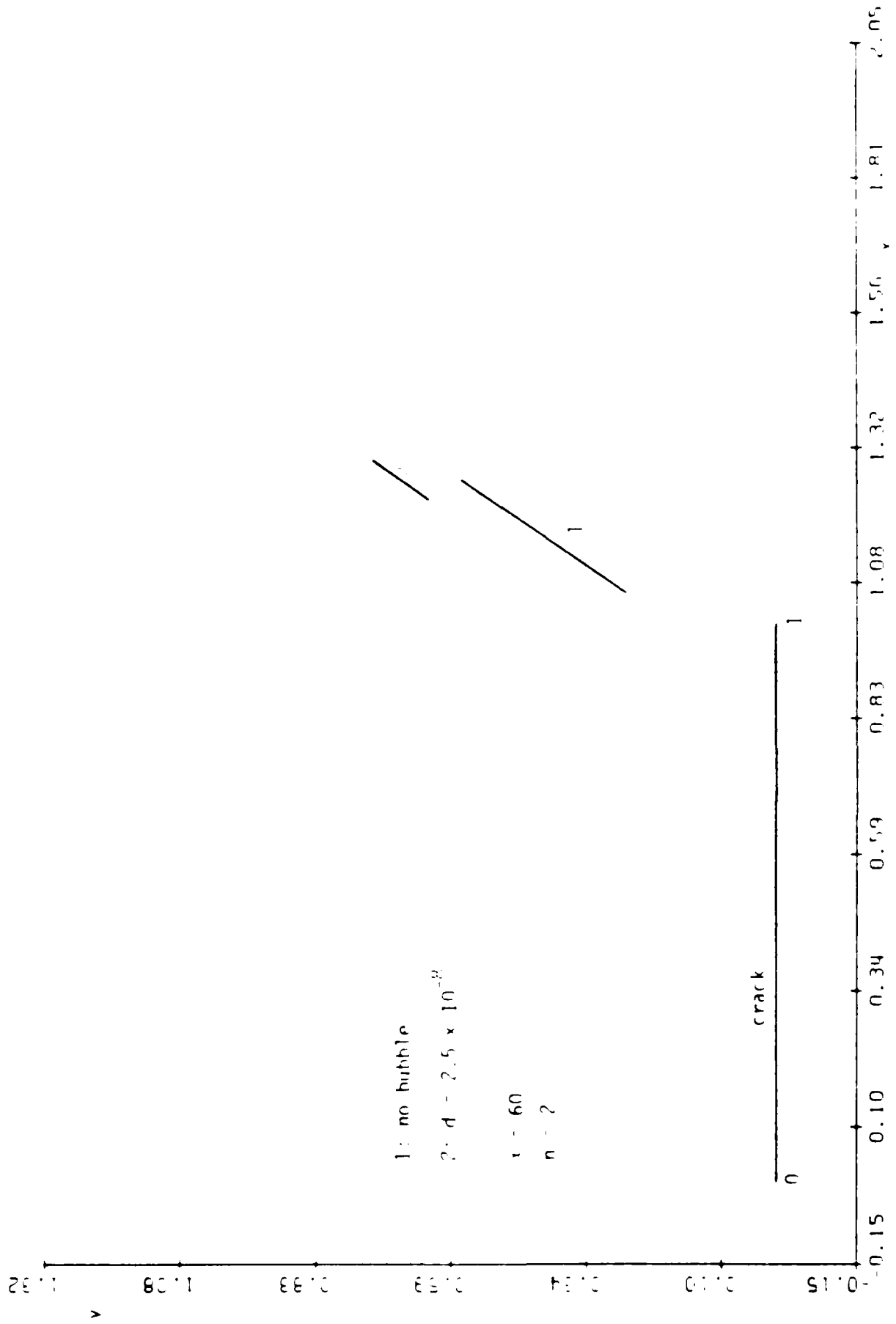
$n = 1$

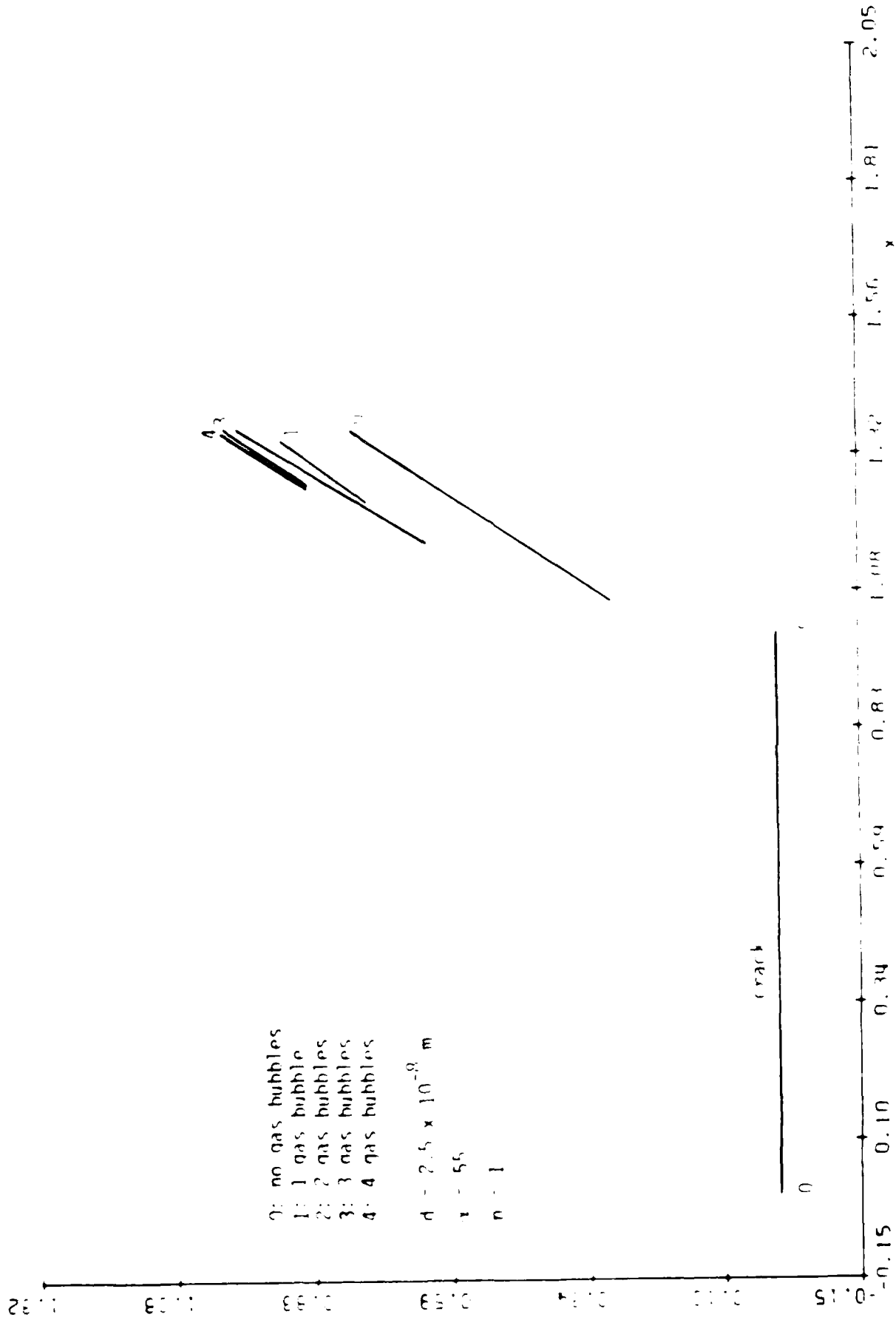
crack

0

c







- 0: no gas bubbles
- 1: 1 gas bubble
- 2: 2 gas bubbles
- 3: 3 gas bubbles
- 4: 4 gas bubbles

$d = 2.5 \times 10^{-8}$ m
 $\gamma = 55$
 $n = 1$

REPORT DOCUMENTATION PAGE		READ INSTRUCTIONS BEFORE COMPLETING FORM
1. REPORT NUMBER ARO 22967.3-EG	2. GOVT ACCESSION NO. AD-A181001	3. RECIPIENT'S CATALOG NUMBER
4. TITLE (and Subtitle) Effect of Gas Bubbles on the Plastic Zone around a Crack Tip		5. TYPE OF REPORT & PERIOD COVERED Technical Report April 1987
		6. PERFORMING ORG. REPORT NUMBER
7. AUTHOR(s) G.D.C. Dhondt A.C. Erinsen		8. CONTRACT OR GRANT NUMBER(s) DAAL03-86-K-0019
9. PERFORMING ORGANIZATION NAME AND ADDRESS Princeton University Princeton, N.J. 08544		10. PROGRAM ELEMENT, PROJECT, TASK AREA & WORK UNIT NUMBERS
11. CONTROLLING OFFICE NAME AND ADDRESS U.S. Army Research Office P.O. Box 12211 Research Triangle Park, N.C. 27709		12. REPORT DATE April 1987
		13. NUMBER OF PAGES
14. MONITORING AGENCY NAME & ADDRESS (if different from Controlling Office)		15. SECURITY CLASS (of this report)
		16a. DECLASSIFICATION/DOWNGRADING SCHEDULE
16. DISTRIBUTION STATEMENT (of this Report) Approved for Public Release-distribution unlimited		
17. DISTRIBUTION STATEMENT (of the abstract entered in Block 20, if different from Report)		
18. SUPPLEMENTARY NOTES The findings of this report are not to be construed as an official Department of the Army position, unless so designated by other authorized documents.		
19. KEY WORDS (Continue on reverse side if necessary and identify by block number) Dislocation, crack, plastic zone; Helium embrittlement		
20. ABSTRACT (Continue on reverse side if necessary and identify by block number) (See reverse for abstract)		

During the loading of a crack edge dislocations are emitted from the crack tip forming a plastic zone. The presence of gas bubbles near the crack tip can change the plastic zone size and location drastically. A detailed study of the force field on an edge dislocation due to the crack load and gas bubbles allows for the determination of the plastic zone as a function of the inclination angle. The dislocation distribution along the plastic zone is found from force equilibrium considerations. Due to the presence of gas bubbles a shrinking and repulsion of the plastic zone from the crack tip is noticed. This process indicates the material embrittlement. The dislocation free zone (DFZ) near the crack tip grows. This embrittlement can become crucial in material design for fusion applications.

END

6-87

DTIC